

Characterization and Design of Digital Pointing Subsystem for Optical Communication Demonstrator

C. Racho, A. Portillo

14 December 1998

Abstract

The Optical Communications Demonstrator (OCD) is a laboratory-based lasercom demonstration terminal designed to validate several key technologies, including beacon acquisition, high bandwidth tracking, precision beam pointing, and point-ahead compensation functions. It has been under active development over the past few years. The instrument uses a CCD array detector for both spatial acquisition and high-bandwidth tracking, and a fiber coupled laser transmitter. The array detector tracking concept provides wide field-of-view acquisition and permits effective platform jitter compensation and point-ahead control using only one steering mirror. This paper describes the detailed design and characterization of the digital control loop system which includes the Fast Steering Mirror (FSM), the CCD image tracker, and the associated electronics. The objective is to improve the overall system performance using laboratory measured data.

The design of the digital control loop is based on a linear time invariant open loop model. The closed loop performance is predicted using the theoretical model. With the digital filter programmed into the OCD control software, data is collected to verify the predictions. This paper presents the results of the system modeling and performance analysis. It has been shown that measurement data closely matches theoretical predictions.

An important part of the laser communication experiment is the ability of FSM to track the laser beacon within the required tolerances. The pointing must be maintained to an accuracy that is much smaller than the transmit signal beamwidth. For an earth orbit distance, the system must be able to track the receiving station to within a few microradians. The failure to do so will result in a severely degraded system performance.

1 Introduction

The goals of this effort are to characterize the end-to-end system performance of the digital controller for the Optical Communication Demonstrator and to prepare for the upgrade of the Fast Steering Mirror that could substantially improve the pointing accuracy. To improve the pointing accuracy, the existing system software was modified to collect data which could characterize the FSM, the FSM electronics, and the camera imaging subsystem. The system is measured in both open loop and closed loop operating modes. A linear time invariant open loop model is developed and is used in the design of a compensating digital filter. The closed loop performance is predicted using MATLAB. With the digital filter programmed into the OCD control software, data is collected to verify the predictions. This paper presents the results of the system modeling and performance analysis.

2 Laboratory Measurements

2.1 Hardware

The OCD design is described in detail in [4]. For the purposes of analyzing the mirror control system to improve the laser beacon tracking, the system is grouped conceptually into subsystems.

The OCD forward loop consists of the DSP which runs the control and imaging software, the DAC which converts the digital filter signal to an analog input signal for the FSM servo, and the two axis FSM servo and mirror. The FSM position sensor is a CCD which reports a centroid value derived from the CCD image. The DAC, FSM servo, and mirror are treated as the system plant. The CCD is treated as elements which only contributes to the system delay within the target control loop bandwidth of 100 Hz and are modeled as such. This does not mean however that it is the only element in the loop which contribute to the system delay. The DSP and the DSP software are considered to make up the digital filter.

2.2 Data Collection

The OCD FSM control law is implemented on a Texas Instruments TMS320C44 Digital Signal Processor (DSP). All system code changes, i.e., software written and compiled to run on the DSP, and all data capture are accomplished by way of the Signalogic(tn) digital signal processing development environment. The data collected for these experiments were obtained at a real-time system rate of 2KHz. This system can buffer data sequences of up to 4000 points long.

Data gathered for the mirror operating in open loop mode was accomplished by inputting a known signal, such as a sine wave, into the OCD Fast Steering Mirror(FSM) control driver circuitry. The open loop data was collected for two input cases, a sine wave and a white noise signal. These input digital signals were generated in the DSP software. Each digital input point represents the desired or commanded centroid pixel location which is essentially how mirror position is measured. The FSM positions were then determined by reading the CCD camera calculated centroid values for both the Mirror X- and Y- axes. The values collected for these experiments consisted of the generated input centroid signal and the calculated centroid results from the CCD camera.

In closed loop operation, the loop is closed around a compensating digital filter. The mirror position, i.e. the centroid calculation, is fed back and subtracted from the desired position. This error is then input to the filter in order to produce the mirror control signal which is applied to the FSM driver control circuit. In the closed loop mode, a sine wave signal was applied in a way similar to the open loop method. However, the compensator drives the mirror in an attempt to track the sinusoid input. The input signal and the feedback centroid information are simultaneously recorded at the sample rate of 2 KHz.

In either open or closed loop mode, the data was obtained for selected discrete input sine wave frequencies. For open loop mode, the white noise input was generated by creating a DC signal where the level is fixed for a given number of sample intervals and is determined by a random number generator. The update rate for the latter signal was 1 KHz, i.e the level is fixed for two samples, with a sequence length of 2000 points.

3 Open Loop Characterization

A model for the open loop mirror was developed for each axis of the mirror position controller. A white noise signal was injected into the open loop mirror control system at the input to the loop, see Figure 1. The digital output and input data was saved to a file and then analyzed in the frequency domain using MATLAB. The procedure used to estimate the frequency response function is described in Section 9. In addition, digital sine waves at selected discrete frequencies were input to the open loop system and the data recorded. The magnitude and phase data for both the white noise and sine wave inputs were plotted for each axis. As expected the two sets of data agree as shown in Figure 2 and Figure 3.

A second order linear time invariant model was derived empirically using MATLAB by fitting the open loop data in both amplitude and phase. The dotted lines which coincide with the measured

responses in Figure 2 and Figure 3 are the bode plots of the resulting MATLAB models.

The X-Axis Mirror Plant Model, $M_x(s)$ in Equation 1, has a double pole estimated to be at 18.5 Hertz with a damping ratio of 0.5. The Y-Axis Mirror Plant Model, $M_y(s)$ in Equation 2, has a double pole estimated to be at 19 Hz with a damping ratio of 0.45.

$$M_x(s) = \frac{13500}{s^2 + 37 * 2\pi * 0.5s + (18.5 * 2\pi)^2} \quad (1)$$

$$M_y(s) = \frac{13900}{s^2 + 38 * 2\pi * 0.45s + (19 * 2\pi)^2} \quad (2)$$

The additional phase delay attributed to any time delays in the loop, e.g. calculating the new centroid, is linearly modeled by $H_x(s)$ in Equation 3 and $H_y(s)$ in Equation 4.

$$H_x(s) = \frac{-s + \frac{2}{T_{dx}}}{s + \frac{2}{T_{dx}}} \quad (3)$$

Where $T_{dx}=0.00166$.

$$H_y(s) = \frac{-s + \frac{2}{T_{dy}}}{s + \frac{2}{T_{dy}}} \quad (4)$$

Where $T_{dy}=0.00125$.

The resulting modeled open loop system phase delay can be seen in Figure 4 and Figure 5 along with the measured open loop system phase delay data. The fitting parameters such as gain, phase delay, poles, and damping ratio of the linear model are varied such that the norm of magnitude and phase of the estimated transfer function minus the fitted transfer is minimized.

4 Closed Loop Prediction

Using the MATLAB open loop plant model, the loop was closed around a continuous time equivalent of the digital filter designed by B. Lurie and S. Sirlin [3]. The digital filters are included below in Equation 5 and Equation 6 and are documented in their memo dated January 29, 1997. The design is based on pole-zero cancellation or pole shifting where the stable poles of the plant are cancelled by zeros of the digital filter and replaced with poles in more desirable locations [2]. The conversion of the linear systems from continuous time to discrete time domain and vice versa assumes a sampling interval of 2 KHz. The closed loop system for each axis is diagramed in Figure 6 and Figure 7. The frequency domain plots for phase and amplitude of this closed loop system predicted by the MATLAB models are shown in Figure 8, Figure 9, Figure 10, and Figure 11. The X-Axis digital filter, $C_x(z)$, was modified slightly to account for the different X-Axis plant poles.

$$C_x(z) = \frac{40[1 - 1.9403z^{-1} + 0.9435z^{-2}]}{1 - 1.1765z^{-1} + 0.1765z^{-2}} \quad (5)$$

$$C_y(z) = \frac{48.39[1 - 1.9435z^{-1} + 0.9465z^{-2}]}{1 - 1.1765z^{-1} + 0.1765z^{-2}} \quad (6)$$

The digital filter equations were converted to their equivalent continuous time representation in the Laplace domain, see Equation 7 and Equation 8

$$C_x(s) = \frac{66.02s^2 + 7674.5s + 892137.7}{s^2 + 2799.8s - 1.24337e - 9} \quad (7)$$

	X-Axis		Y-Axis	
	Measured	Predicted	Measured	Predicted
-3dB BW (Magnitude)	128.6 Hz	146 Hz	112.6 Hz	177 Hz
Phase at f= 100Hz	-126 degrees	-138 degrees	-126 degrees	-110 degrees

Table 1: OCD Mirror Closed Position Loop Measured and Predicted Results

$$C_y(s) = \frac{80s^2 + 8810s + 979180}{s^2 + 2799.8s - 1.24337e - 9} \quad (8)$$

The open loop transfer function which includes the compensating filters is used to determine the gain and phase margins for each axis. The open loop bode plots for the x-axis transfer function, $C_x(s)G_x(s)H_x(s)$, and the y-axis transfer function, $C_y(s)G_y(s)H_y(s)$, are shown in figure 14. The resulting x-axis gain and phase margin are 2.895 and 53.73 degrees. Similarly, the y-axis gain and phase margin are 2.9404 and 53.41 degrees. These margins provide for a measure of the system stability.

5 Closed Loop Verification

Experimental data was taken to characterize the closed loop performance with the digital filters in place. The OCD mirror control system was closed around the digital filters in Equation 5 and Equation 6 which were implemented in the OCD software. The filter gains were adjusted separately for each axis in the math models to achieve approximately 100 Hz of control bandwidth. The closed loop system was then tested to verify the math model predictions. Sine waves at discrete frequencies and steps were input as position commands into the closed loop mirror position control system. Each axis was tested independently. The empirical results are shown in the bode and time domain plots along side the predictions in Figures 8-13. For the Y-axis closed loop control, the predicted magnitude response -3 dB bandwidth was near 177 Hz, but the actual turned out to be slightly over 110 Hz, Figure 9. For the X-axis closed loop control, the predicted -3 dB bandwidth was slightly over 146 Hz and the measured was well over 100 Hz, Figure 8. The Y-Axis predicted phase delay at 100 Hz was about -110 degrees, Figure 11. The Y-Axis measured phase delay at 100 Hz was -126 degrees, a 14.5 % difference between predicted and measured. The X-Axis predicted phase delay is -138 degrees and the measured phase delay was -126 degrees which is about 9 % better than predicted, Figure 10. These results are listed in Table 1.

The discrepancy between the predicted and the measured curves at the higher frequencies, above 50 Hz by inspection, indicates that there are some non-negligible nonlinear effects in the real system.

The ratios of input over error for sine wave inputs at discrete frequencies were plotted along with the predicted input over error ratio based on the MATLAB model, see Figure 15 and Figure 16. The transfer functions used to derive the predicted $\frac{U(s)}{E(s)}$ frequency domain responses are shown in Equation 9 and Equation 10.

$$\frac{U_x(s)}{E_x(s)} = 1 + C_x(s)M_x(s)H_x(s) \quad (9)$$

$$\frac{U_y(s)}{E_y(s)} = 1 + C_y(s)M_y(s)H_y(s) \quad (10)$$

6 MATLAB Model Based Predictions

We want to predict system performance for a different mirror and different mirror drives. Assuming the new mirror can be characterized well by a second order linear system, a MATLAB model was created for a mirror plant where the first resonant frequency is $\omega_n=50$ Hertz with damping, $\xi = 0.5$.

Three separate cases are analyzed, the new mirror with no delay added, a second with a one sample interval delay added, and the third with approximately a three sample interval delay. Here, the sample interval is assumed to be 0.0005 second. The latter case is the delay which is present in the current system. The two cases with delay are modeled with the delay in the feedback path. Since this is a theoretical exercise, it is assumed that both axes of the new mirror are identical and not coupled. Hence, we will not be specific in terms of x- and y- axes. The proposed new mirror plant model is given in Equation 11. The digital filter, $C(z)$ in Equation 12, is designed using stable plant pole cancellation as was done for the existing digital filter discussed in the previous sections.

$$M(s) = \frac{99000}{s^2 + 100 * 2\pi * 0.5s + (50 * 2\pi)^2} \quad (11)$$

$$C(z) = \frac{A[1 - 1.8318z^{-1} + 0.8546z^{-2}]}{1 - (1 + P_c)^{-1} + P_c z^{-2}} \quad (12)$$

Where P_c is chosen to be a real valued number less than 1.0 and the choice for A, the forward gain, is a tradeoff between system bandwidth and overshoot.

The digital filter equation was converted to their equivalent continuous time representation in the Laplace domain, see Equation 13. The performance was then analyzed using continuous time domain techniques.

For $P_c = 0.08$,

$$C(s) = \frac{A[s^2 + 3755.3s - 8195879.6]}{s^2 + 5051.4s - 1.5621e - 7} \quad (13)$$

The delays are modeled by the transfer function H_i where $i =$ the number of samples delay.

$$H_0(s) = 1 \quad (14)$$

$$H_1(s) = \frac{-s + 4000}{s + 4000} \quad (15)$$

$$H_3(s) = \frac{-s + 1200}{s + 1200} \quad (16)$$

The closed loop transfer function then becomes

$$\frac{Y(s)}{U(s)} = \frac{A \cdot C(s)M(s)H_i(s)}{1 + A \cdot C(s)M(s)H_i(s)} \quad (17)$$

Where $i = 0,1,$ or 3 .

For the case where there is no delay in the system, $H_0(s)$, we choose $A = 80$ and $P_c = 0.08$ for the digital filter values. The closed loop system response then indicates a 21.8% maximum overshoot and a -3dB bandwidth of approximately 900 Hertz.

If we add in a one sample delay modeled by $H_1(s)$, then choose $A = 20$ and $P_c = 0.08$, the closed loop response results in a maximum overshoot of 29% and a -3dB bandwidth of approximately 373 Hertz.

Controller Values			Results			
	A	P_c	f_{-3dB}	Max O.S.	Phase Margin	Gain Margin
No Delay, H_0	80	0.08	903 Hz	21.8%	48.76 deg	4051.2
1 Sample Delay, H_1	20	0.08	373 Hz	29%	46.98 deg	2.61
3 Sample Delay, H_3	8	0.08	178 Hz	32.8%	47.09 deg	2.39

Table 2: OCD Mirror Closed Position Loop Predicted Results

For the three sample delay, $H_3(s)$, the choice of $A = 8$ and $P_c = 0.08$ results in a closed loop response with a maximum overshoot of 32.8% and a -3dB bandwidth near 183 Hertz. Table 2 summarizes these results. Figures 16 and 17 show the closed loop magnitude and phase response for all three cases. Notice that to maintain a similar phase margin and maximum overshoot for all three cases that the forward gain and bandwidth are reduced significantly as the delay increases.

In addition to the frequency domain characteristics of predicted system discussed above, the time domain error responses due to a step input are plotted and shown in figure 18. The increasing overshoot and settling times demonstrates the difference in tracking performance between the three cases.

7 Summary

This paper characterizes the end-to-end digital control system performance for the OCD. The frequency domain characteristics of both the compensated and uncompensated system were measured and modeled. Also, the time domain response of the closed loop system was simulated and compared to the measured response. A model based analytical tool for performance prediction was developed for the OCD. This model was then used to predict performance for a new mirror. From the model and model-based simulations, we are able to deduce the effects of system delays on system performance. The real system was also modified to generate digital test inputs and allow for measurements to be easily gathered. Hence, the ability to collect real performance data is now part of the system. This feature provides for a systematic approach to quantify any future upgrades to the OCD.

8 Acknowledgments

This work was carried out by the Jet Propulsion Laboratory, California Institutes of Technology, under contract with the National Aeronautics and Space Administration. MATLAB is a registered trademark of The Math Works, Inc. The authors would like to thank...

References

- [1] Charles L. Phillips, H. Troy Nagle, *Digital Control System Analysis and Design, 2nd Edition*. Prentice Hall, 1990.
- [2] Bahram Shahian, Michael Hassul, *Control System Design Using MATLAB*, Prentice Hall, 1993.
- [3] Boris Lurie, Sam Sirlin, "Subject: Optical Communication Controller." Jet Propulsion Laboratory, Interoffice Memorandum to Muthu Jeganathan, Jan. 1997.
- [4] Tsun-Yee Yan, Muthu Jeganathan, James R. Lesh, "Progress on the Development of the Optical Communications Demonstrator", *Free Space Laser Communication Technologies IX, SPIE Proceedings*, Feb. 1997.

- [5] H. Ansari, "Digital Control Design of a CCD-Based Tracking Loop For Precision Beam Pointing", Free Space Laser Communication Technologies VI, SPIE Proceedings, Vol.2123, Jan, 1994.
- [6] Julius S. Bendat, Allan G. Piersol, *Random Data: Analysis and Measurement Procedures, 2nd Edition*, John Wiley & Sons, 1986.

9 Appendix A

The following data analysis procedure is taken from [6].

The time series input data, $x(mt_s)$, and output data, $y(mt_s)$, m a positive integer and t_s the sampling time, are detrended. Next, the data is passed through a Hanning filter to prevent spectral leakage in the Fourier domain.

The magnitude and phase response of the system are estimated using the detrended filtered time series data.

The frequency response estimate for a single-input/single-output system is calculated using the following equations.

$$\hat{H}_{xy}(f) = \frac{\hat{G}_{xy}(f)}{\hat{G}_{xx}(f)} = |\hat{H}_{xy}(f)|e^{-j\phi(f)} \quad (18)$$

where

$$\hat{G}_{xy}(f) = \frac{2}{N_d T} \sum_{i=1}^{N_d} X_i(f, T) \cdot Y_i^*(f, T) \quad (19)$$

is the averaged estimate of the one-sided cross-spectral density and

$$\hat{G}_{xx}(f) = \frac{2}{N_d T} \sum_{i=1}^{N_d} |X_i(f, T)|^2 \quad (20)$$

is the averaged estimate of the one-sided auto-spectral density.

$T = Nt_s$, Length of the data subrecord in seconds N = Number of data points in the data subrecord

$T_r = N_d T$, Total record length of the data in seconds

N_d = Number of distinct and disjoint subrecords of length T seconds in the total record.

t_s = Sampling time

$X_i(f, T)$ =Finite Fourier transform of the i th subrecord of the time series data, $x(mt_s)$ and

$Y_i(f, T)$ =Finite Fourier transform of the i th subrecord of the time series data, $y(mt_s)$

The system magnitude response = $|\hat{H}_{xy}(f)|$ and the system phase response is $\hat{\phi}(f)$. The estimated transfer function has values at the following discrete frequencies $f = f_k$ where $f_k = \frac{k}{Nt_s}$, for $k = 0, \dots, \frac{N}{2}$

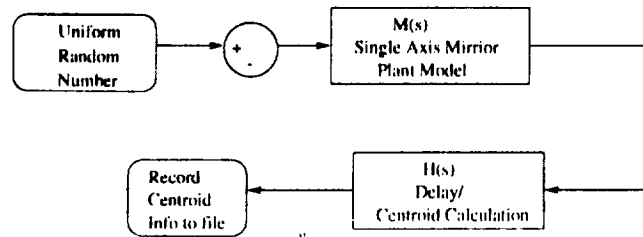


Figure 1: OCD Mirror Open Loop Plant Modeling Block Diagram, Continuous Time.

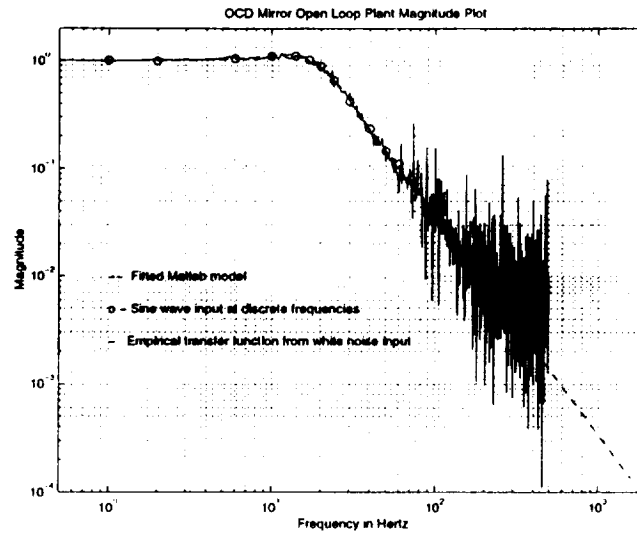


Figure 2: OCD Mirror Open Loop X-Axis Magnitude Data Plot

10 Figures

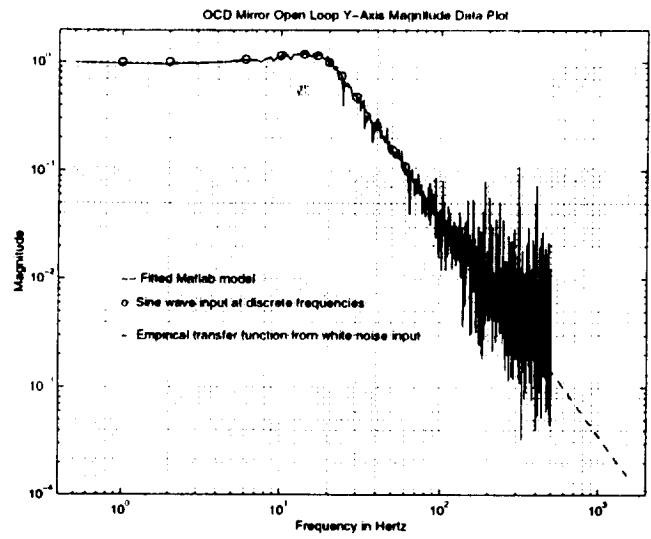


Figure 3: OCD Mirror Open Loop Y-Axis Magnitude Data Plot

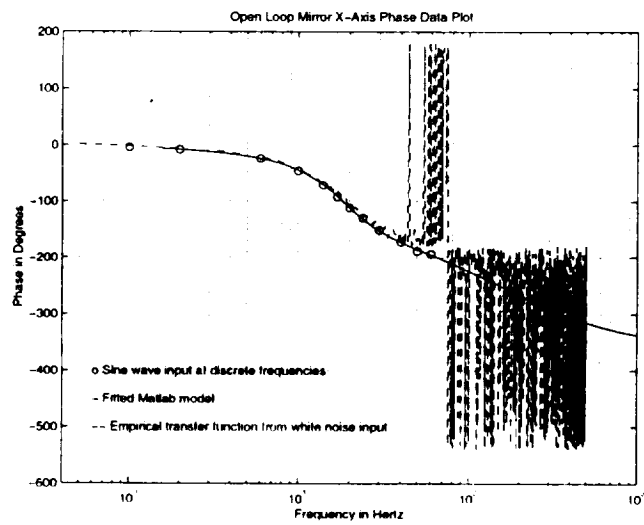


Figure 4: OCD Mirror Open Loop X-Axis Phase Data Plot

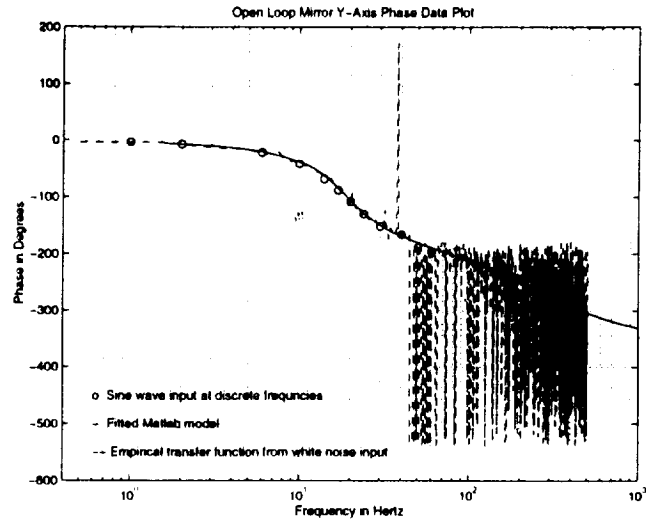


Figure 5: OCD Mirror Open Loop Y-Axis Phase Data Plot

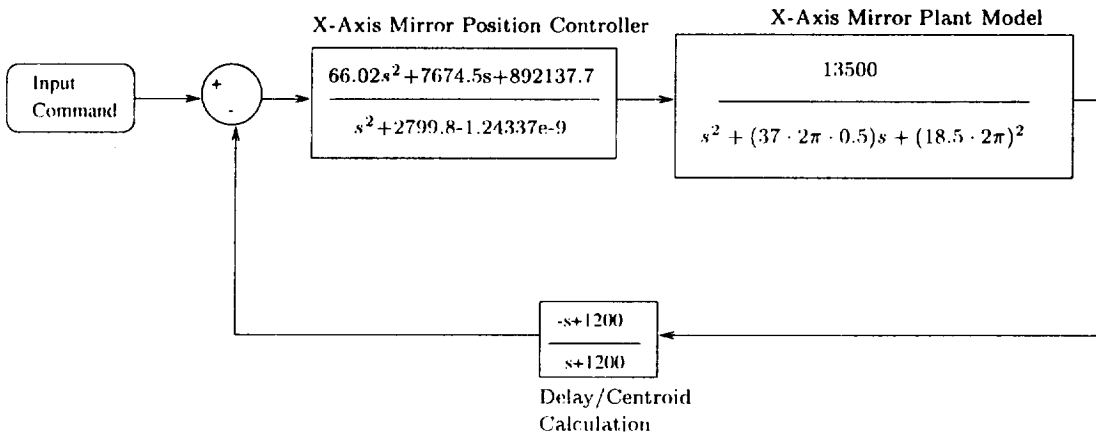


Figure 6: OCD X-Axis Mirror Closed Loop Control Block Diagram, Continuous Time.

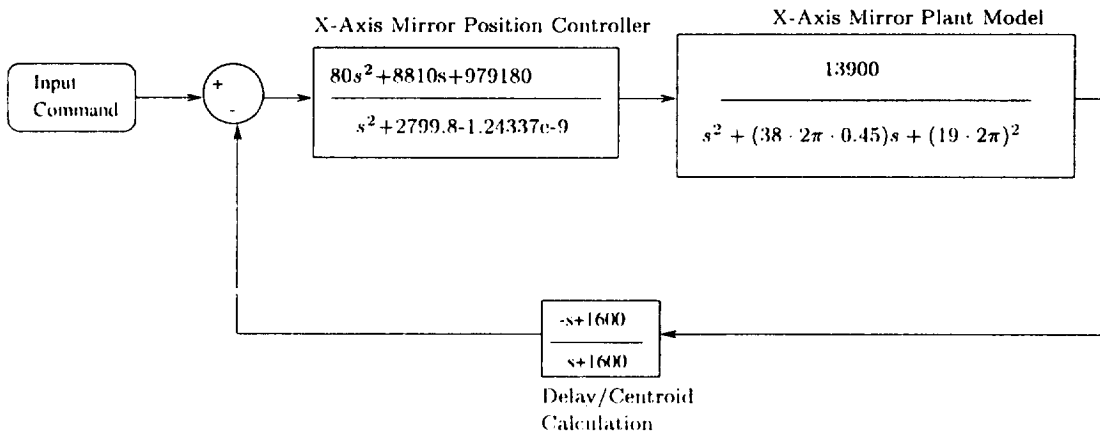


Figure 7: OCD X-Axis Mirror Closed Loop Control Block Diagram, Continuous Time.

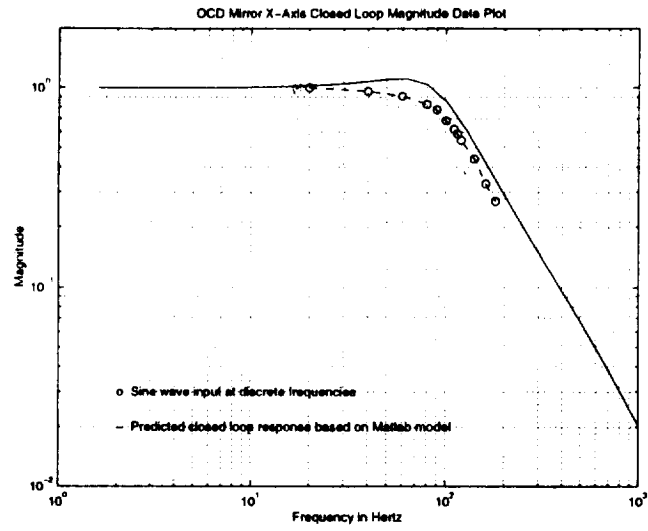


Figure 8: OCD Mirror X-Axis Closed Loop Magnitude Data Plot

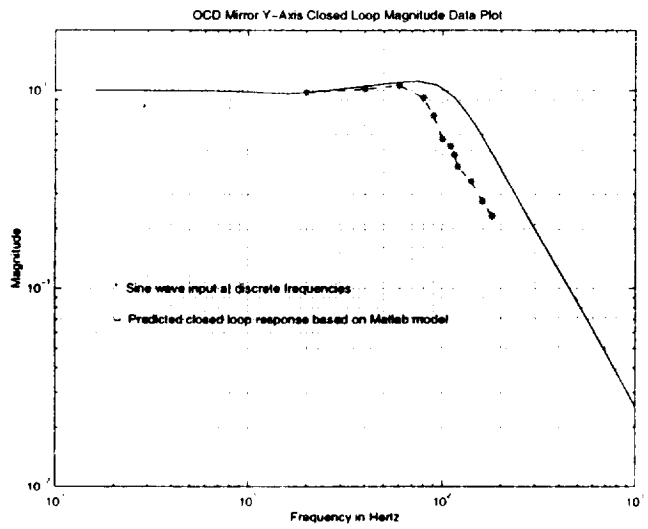


Figure 9: OCD Mirror Y-Axis Closed Loop Magnitude Data Plot

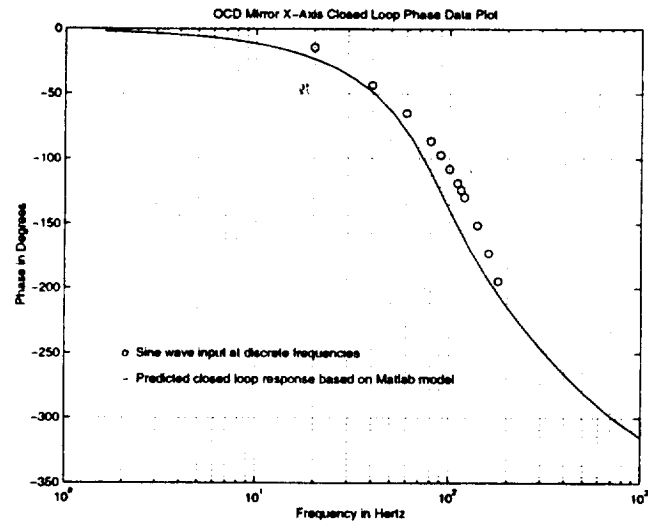


Figure 10: OCD Mirror X-Axis Closed Loop Phase Data Plot

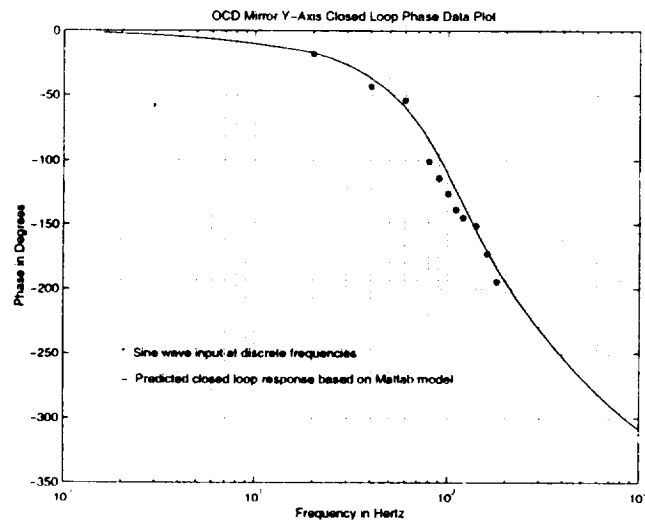


Figure 11: OCD Mirror Y-Axis Closed Loop Phase Data Plot

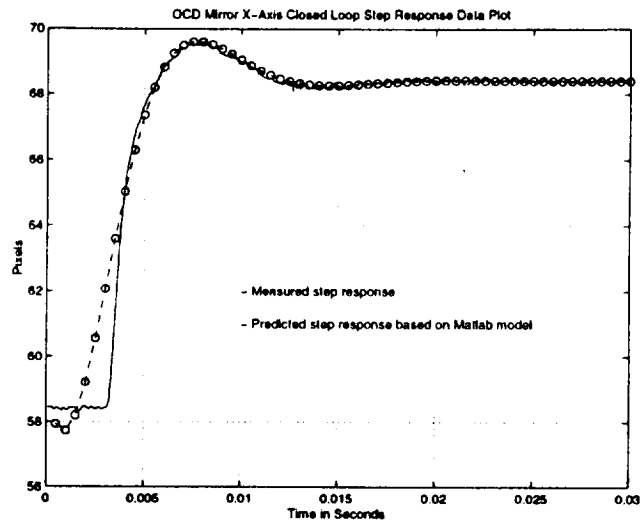


Figure 12: OCD Mirror X-Axis Closed Loop Step Response Data Plot

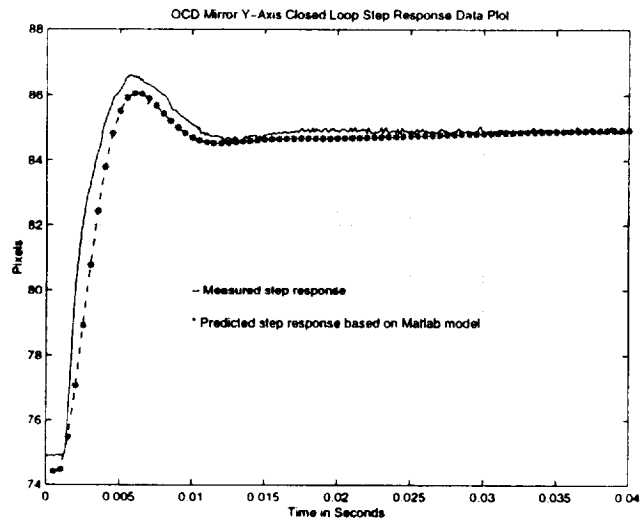


Figure 13: OCD Mirror Y-Axis Closed Loop Step Response Data Plot

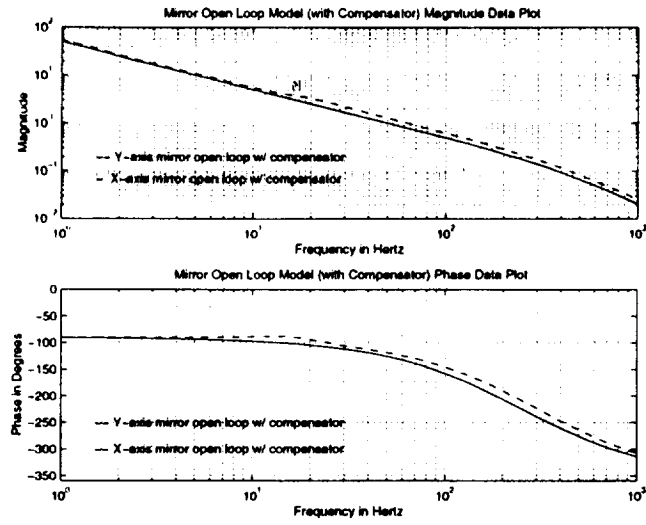


Figure 14: OCD Mirror Open Loop Model with Compensator Magnitude and Phase Data Plot

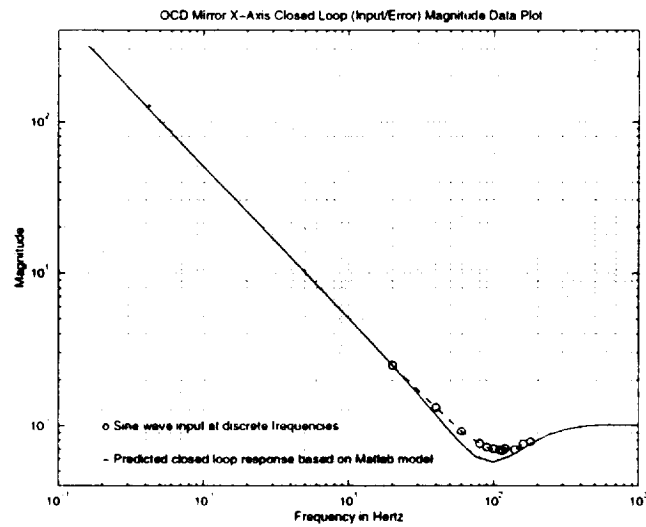


Figure 15: OCD Mirror X-Axis Closed Loop (Input/Error) Magnitude Data Plot

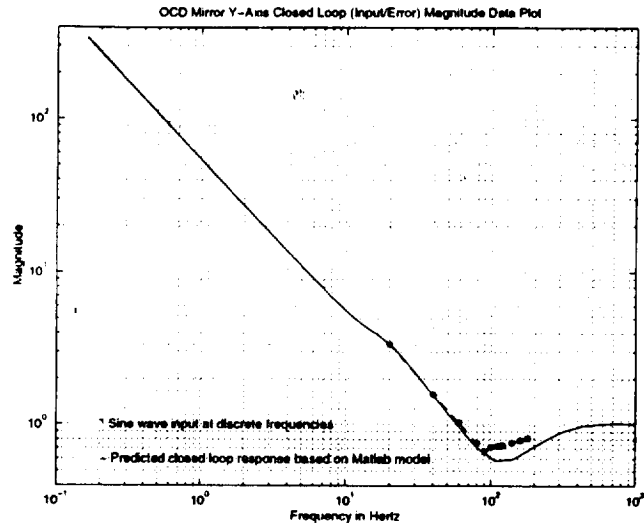


Figure 16: OCD Mirror Y-Axis Closed Loop (Input/Error) Magnitude Data Plot

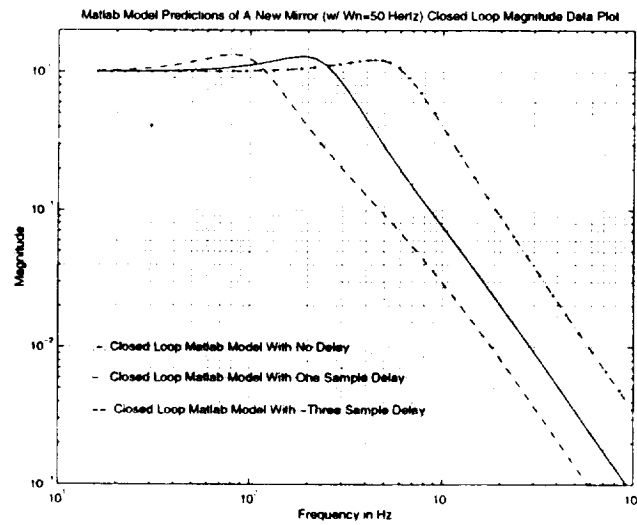


Figure 17: MATLAB Model Predictions Of A New Mirror($\omega_n = 50$ Hertz) Closed Loop Magnitude Data Plot.

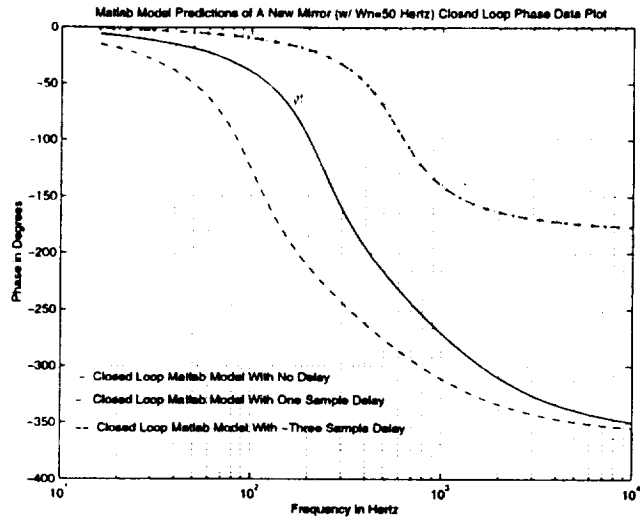


Figure 18: MATLAB Model Predictions Of A New Mirror($w/ \omega_n = 50$ Hertz) Closed Loop Phase Data Plot.

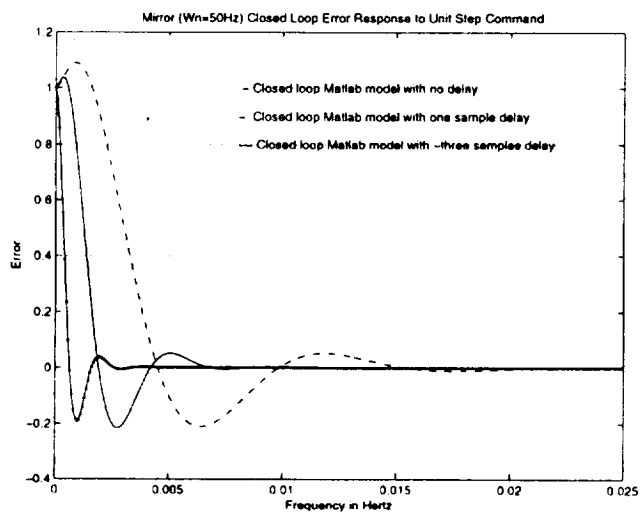


Figure 19: MATLAB Model Predictions Of A New Mirror($w/ \omega_n = 50$ Hertz) Closed Loop Error Response to Step Input.